STA2503 Project 1: American Options

October 31, 2023

Reilly Pickard, Willem Atack & Brandon Tam

Abstract

This study aims to synthesize the theoretical constructs of no-arbitrage financial markets, self-financing strategies, and replicating portfolios in the context of American put options. Within this investigation, a comprehensive analysis of put option pricing, the delineation of decision boundaries, and the composition of hedging portfolios is described. The analysis is conducted within the framework of a discrete-time model, which has been adapted from the seminal Cox, Ross, Rubenstein model. Moreover, the study employs computational implementation, facilitated through the Python programming language, to compute the optimal exercise boundary for the American put option for a variety of parameter combinations. The dynamics of profit and the associated stopping times for put option positions under diverse market conditions are then examined through computational simulation. The results displayed that heightened market volatility leads to an augmentation in the valuation of American put options while concurrently causing a decrement in the exercise boundary. In contrast, an escalation in risk-free interest rates results in a depreciation of American put option value and an elevation of the exercise boundary.

Introduction

Financial derivatives are instruments whose value is derived by some underlying process. An example is an American put option, whose payoff value is the maximum of the difference between some predefined strike price and the underlying asset value, and zero. An American put is said to be exercised when the holder takes the payoff at some time before the maturity date. As these tradeable options play a large role in the financial industry, a profound grasp of the nuanced features inherent to these options, encompassing their pricing mechanisms, the definition of optimal exercise boundaries, and the formulation of replicating portfolios, stands as a vital imperative for financial practitioners. A knowledge in how these instruments are valued and specifically how their value is impacted by market parameters such as the volatility and risk-free rates, are vital for adept management of positions, the strategic generation of potential profit, as well as the prudent hedging of associated risks.

In this report, a discrete-time financial model is used to value American put options, compute optimal exercise boundaries, mitigate risk with a replication strategy, and examine profit and stopping times over multiple simulated paths. To construct this model, consider an American put option written on asset S with the following characteristics:

1. The option expires at time $T > 0$ and has a predetermined strike price K.
2. The underlying asset S follows a discrete time model with $N \in \mathbb{N}^+$ equispaced time steps. The length of each time step is $\Delta t = \frac{T}{N}$. $S = (S_{t_k})$ is the asset price stochastic process, where $k \in \{1, ..., N\}$ and $t_k = k\Delta t$. The stochasticity introduces risk to this process, and S will be referred to as the risky asset in this market.
3. The volatility of S is given by a constant $\sigma > 0$, and its drift is given by a constant $\mu \in \mathbb{R}$. The dynamics of S are given by $S_{t_k} = S_{t_{k-1}} e^{r\Delta t + \sigma\sqrt{\Delta t}\epsilon_k}$, where ϵ_k are i.i.d. random variables with $\epsilon_k \in \{-1, 1\}$ and $\mathbb{P}(\epsilon_k = \pm 1) = \frac{1}{2}(1 \pm \frac{(\mu - r) - 0.5\sigma^2}{\sigma}\sqrt{\Delta t})$

4. In addition to S, the market consists of a bank account process B_t which accumulates interest at a continuously compounded risk free rate $r \geq 0$. That is, $B_t = e^{rt}$ for all $t \geq 0$.

The report is organized as follows: first, the risk-free martingale measure is derived by ensuring the market admits no arbitrage. Using this martingale measure, the valuation and replication processes of an American option is highlighted, and the distribution of the log returns as the number of discrete time steps goes to infinity is examined. The derived model is then implemented. Prices and exercise boundaries for multiple volatility-rate combinations are computed and visualized, along with the corresponding replication hedging strategies. Finally, 10,000 price paths of asset S are simulated, and the corresponding profit and stopping time distributions are analyzed. This is repeated for various different risk-free rates and volatilities, and the final portion of the study examines the case where the realized volatility differs from the volatility which is used to price the option.

Part 1: Theory

Martingale Measure with the Bank Account as the Numeraire

Because the price of asset S either moves up or down at each time step, the relative price process of the risky asset with B_t as the numeraire, $\frac{S_t}{B_t}$, may be modelled as a binomial tree. Figure 1 shows the evolution from the initial position to the first time step. The fundamental theorem of asset pricing can be used to deduce branching probabilities given by the equivalent martingale measure $\mathbb{Q}$.

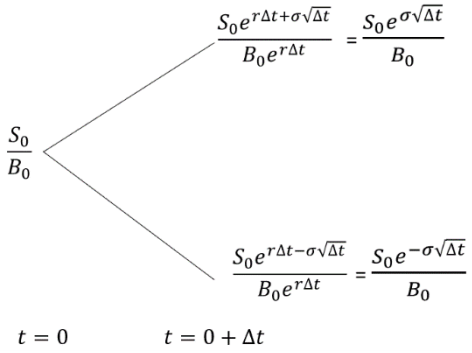

Figure 1: Evolution of $\frac{S_t}{B_t}$ from $t = 0$ to $t = \Delta t$

The fundamental theorem of asset pricing states that if there is no arbitrage, then there exists a probability measure $\mathbb{Q}$ equivalent to $\mathbb{P}$ such that $\mathbb{E}^{\mathbb{Q}}[\frac{S_{t_k}}{B_{t_k}}|\mathcal{F}_{t_{k-1}}] = \frac{S_{t_{k-1}}}{B_{t_{k-1}}}$. From Figure 1 above, it is easy to see that the probability q of reaching the upper branch satisfies equation 1 below.

$$\frac{S_{t_k}}{B_{t_k}} = q\frac{S_{t_{k-1}}e^{\sigma\sqrt{\Delta t}}}{B_{t_{k-1}}} + (1-q)\frac{S_{t_{k-1}}e^{-\sigma\sqrt{\Delta t}}}{B_{t_{k-1}}} \implies q = \frac{1-e^{-\sigma\sqrt{\Delta t}}}{e^{\sigma\sqrt{\Delta t}} - e^{-\sigma\sqrt{\Delta t}}} \tag{1}$$

Now, let $C_{t,i}$ denote the value of an American call option written on S with strike price K. Using the terminal values of the option $C_{T,i} = \max\{0, K - S_{T,i}\}$ for all states i in combination with

the price trees for S and B, one can construct a binomial tree for the relative option value process (denoted $\frac{C_{t_k,i}}{B_{t_k,i}}$) for all possible states i at all possible time steps t_k. At any time t and state i, the option value is the maximum of the intrinsic (exercise) value $\max(0, K - S_{t,i})$ and the value of holding the option until the next state. Using backward induction and the martingale property, it can be shown that the value of holding the option satisfies equation 2 below.

$$\frac{C_{t_k,i}}{B_{t_k,i}} = q\frac{C_{t_{k+1,i}}}{B_{t_{k+1,i}}} + (1-q)\frac{C_{t_{k+1,i+1}}}{B_{t_{k+1,i+1}}} \tag{2}$$

As $\frac{B_{t_{k+1}}}{B_{t_k}} = e^{-r\Delta t}$ for any state i, one can compute the value of the option at each time t and state i as:

$$\max\{K - S_{t,i}, V^{\text{hold}}\},\ V^{\text{hold}} = e^{-r\Delta t}[qC_{t_{k+1},i} + (1-q)C_{t_{k+1},i+1}] \tag{3}$$

Martingale Measure with the Risky Asset as the Numeraire

The relative price process of the risky asset with S_t as the numeraire, $\frac{B_t}{S_t}$ can also be modelled as a binomial tree. Figure 2 shows the evolution from the initial position to the first time step. The fundamental theorem of asset pricing can be used to deduce branching probabilities given by the equivalent martingale measure $\mathbb{Q}^S$.

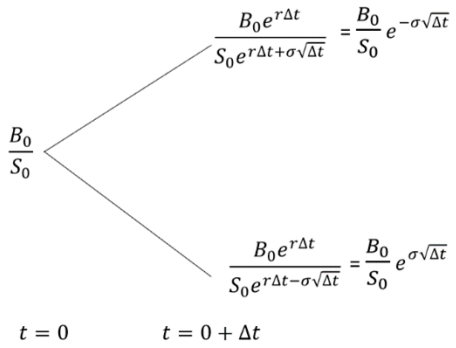

Figure 2: Evolution of $\frac{B_t}{S_t}$ from $t = 0$ to $t = \Delta t$

Again using the fundamental theorem of asset pricing, if there is no arbitrage then there exists a probability measure $\mathbb{Q}^S$ equivalent to $\mathbb{P}$ such that $\mathbb{E}^{\mathbb{Q}^S}[\frac{B_{t_k}}{S_{t_k}}|\mathcal{F}_{t_{k-1}}] = \frac{B_{t_{k-1}}}{S_{t_{k-1}}}$. From Figure 2, the probability q^S of reaching the upper branch satisfies equation 4:

$$\frac{B_{t_k}}{S_{t_k}} = q^S\frac{B_{t_{k-1}}e^{-\sigma\sqrt{\Delta t}}}{S_{t_{k-1}}} + (1-q^S)\frac{B_{t_{k-1}}e^{\sigma\sqrt{\Delta t}}}{S_{t_{k-1}}} \implies q^S = \frac{1 - e^{\sigma\sqrt{\Delta t}}}{e^{-\sigma\sqrt{\Delta t}} - e^{\sigma\sqrt{\Delta t}}} \tag{4}$$

Repeating the option valuation with the risky asset as the numeraire, and the terminal values of the option $C_{T,i} = \max\{0, K - S_{T,i}\}$ for all states i in combination with the price trees for S and

B, one can construct a binomial tree for the relative option value process (denoted $\frac{C_{t_k,i}}{S_{t_k,i}}$) for all possible states i at all possible time steps t_k. Recalling that at any time t and state i, the option value is the maximum of the intrinsic (exercise) value $\max(0, K - S_{t,i})$ and the value of holding the option until the next state. Once again using backward induction and the martingale property, it is shown that the value of holding the option is deduced to:

$$\frac{C_{t_k,i}}{S_{t_k,i}} = q^S \frac{C_{t_{k+1},i}}{S_{t_{k+1},i}} + (1 - q^S) \frac{C_{t_{k+1},i+1}}{S_{t_{k+1},i+1}} \tag{5}$$

Hedging Strategy

Consider an investor who has purchased the described American put option on the underlying asset S. This investor faces the financial risk associated with asset S remaining above the strike price. To mitigate this risk, a position in the underlying asset and the bank account may be used to generate a dynamic hedging strategy.

Let the value of the hedging portfolio θ be represented by $V^\theta = \{V^\theta_{t_k}\}_{k \in \{1,2,\ldots,N\}}$. To create a perfect hedge, we wish for the value of the portfolio at any time t_k to be zero. In other words, moves in option value at time t_k are perfectly offset by the market participant's holdings in the underlying asset and bank account. Thus, if the holdings in S_{t_k}, B_{t_k} and the put option are denoted by $\theta_{t_k} = [\alpha_{t_k},\ \beta_{t_k},\ 1]$ (ie. we hold a long position in the put) and $V^\theta_{t_k} = 0$ for all t_k, then at time t_k:

$$\alpha_{t_k} S_{t_k} + \beta_{t_k} B_{t_k} + C_{t_k} = 0 \implies \beta_{t_k} = -\frac{\alpha_{t_k} S_{t_k} + C_{t_k}}{e^{r t_k}} \tag{6}$$

where C_{t_k} denotes the value of the option at time t_k (which is known at time t_k).

Since $\alpha_{t_k} S_{t_{k+1}} + \beta_{t_k} B_{t_{k+1}}$ must be equal to the negative value of the put option in both states i and $i + 1$, it is concluded that:

$$\alpha_{t_k} = \frac{C_{t_k+1,i+1} - C_{t_k+1,i}}{S_{t_k} e^{r\Delta t}[e^{\sigma\sqrt{\Delta t}} - e^{-\sigma\sqrt{\Delta t}}]} \tag{7}$$

Distribution of the Log Returns

Theorem: Under the model assumptions in the introduction, the distribution of $\ln(\frac{S_T}{S_0})$ converges to a normal distribution with mean rT and variance $\sigma^2 T$ as $N \to \infty$.

Proof: By the model assumptions,

$$\begin{aligned}
\ln(\frac{S_T}{S_0}) &= \ln(\frac{S_{t_N}}{St_{N-1}} \cdots \frac{S_{t_1}}{S_0}) \\
&= \sum_{k=1}^{N} \ln(\frac{S_{t_k}}{S_{t_{k-1}}}) \\
&= \sum_{k=1}^{N} \ln(\frac{S_{t_{k-1}} e^{r\Delta t + \sigma\sqrt{\Delta t}\epsilon_k}}{S_{t_{k-1}}}) \\
&= \sum_{k=1}^{N} r\Delta t + \sigma\sqrt{\Delta t}\epsilon_k \\
&= rT + \sigma\sqrt{\Delta t}\sum_{k=1}^{N} \epsilon_k
\end{aligned}$$

So, the moment generating function of $\ln(\frac{S_T}{S_0})$ is given by,

$$\begin{aligned}
E[e^{(rT+\sigma\sqrt{\Delta t}\sum_{k=1}^{N}\epsilon_k)z}] &= E[e^{zrT}e^{z\sigma\sqrt{\Delta t}\sum_{k=1}^{N}\epsilon_k}] \\
&= e^{zrT}(E[e^{z\sigma\sqrt{\Delta t}\epsilon_1}])^N
\end{aligned}$$

where the last equality follows from the fact that the ϵ_i are i.i.d.

By definition of $\mathbb{P}$, $E[e^{z\sigma\sqrt{\Delta t}\epsilon_1}] = \frac{1}{2}e^{z\sigma\sqrt{\Delta t}}(1 + \frac{(\mu-r)-0.5\sigma^2}{\sigma}\sqrt{\Delta t}) + \frac{1}{2}e^{-z\sigma\sqrt{\Delta t}}(1 - \frac{(\mu-r)-0.5\sigma^2}{\sigma}\sqrt{\Delta t})$.

As $\Delta t \to 0$, the expectation above converges to $\cosh(z\sigma\sqrt{\frac{T}{N}})$. Thus, it suffices to show that $[\cosh(z\sigma\sqrt{\frac{T}{N}})]^N \to e^{\frac{1}{2}\sigma^2 T z^2}$ as $N \to \infty$.

Let $u = z\sigma\sqrt{T}$. Then, using the Taylor expansions of $\cosh(x)$ and $\ln(1+x)$,

$$\begin{aligned}
\lim_{N\to\infty}[\cosh(z\sigma\sqrt{\frac{T}{N}})]^N &= e^{\lim_{N\to\infty}[N\ln(\cosh(\frac{u}{\sqrt{N}}))]} \\
&= e^{\lim_{N\to\infty}[N\ln(1+\frac{u^2}{2N}+\mathcal{O}(\frac{1}{N}))]} \\
&= e^{\lim_{N\to\infty}[N(\frac{u^2}{2N}+\mathcal{O}(\frac{1}{N})+\mathcal{O}(\frac{1}{N}))]} \\
&= e^{\lim_{N\to\infty}[\frac{u^2}{2}+\mathcal{O}(1)]} \\
&= e^{\frac{u^2}{2}} \\
&= e^{\frac{1}{2}\sigma^2 T z^2}
\end{aligned}$$

■

Part 2: Description of Implementation and Interpretation

Option Price and Exercise Boundary Calculation

The backward induction described in the previous section was implemented computationally with Python twice (once for each numeraire choice). Figure 3 below shows the optimal exercise boundary for $N = 5000, S_0 = \$10.00, K = \$10.00, r = 0.02, \sigma = 0.2, \mu = 0.05$ and $T = 1$, where the variables are as defined in the introduction. The figure shows that the exercise boundary when the bank account is used as the numeraire (left) and the exercise boundary when the risky asset is used as the numeraire (right) are identical. In both cases, the option premium is calculated to be \$0.71. As the implementation with both numeraires produced the same results, the remaining analysis was done with the bank account as the numeraire.

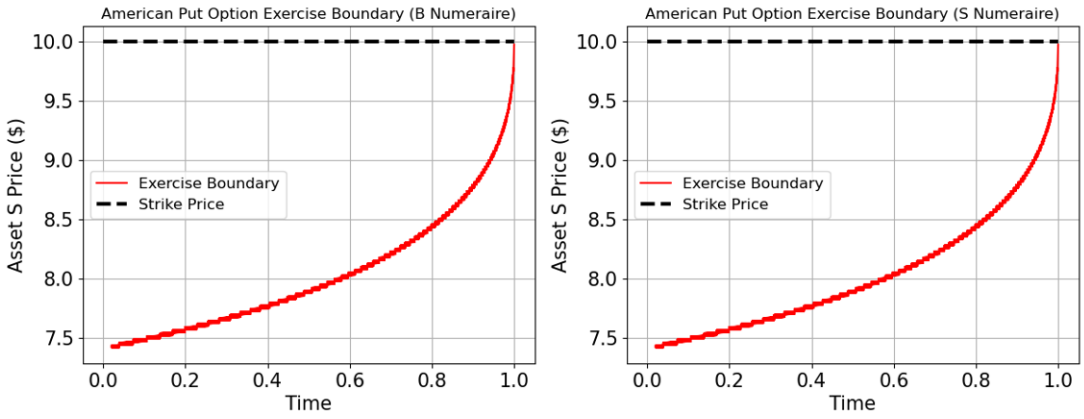

Figure 3: Exercise Boundaries for an American Put Option when S and B are used as Numeraires

Hedging Strategy

To illustrate the risky asset processes and their respective interactions with the boundary, two simulated paths of the asset S (using the same parameters as the previous figure) are shown in Figure 4. One path never crosses the exercise boundary, and one path crosses the exercise boundary at $t \approx 0.7$.

Using equations 6 and 7, the hedging strategy of an investor who bought the put option can be computed path wise. Figure 5 shows the positions the investor would take in asset S and the bank account for both paths shown in Figure 4. Recalling that the investor took a long position in the put option, the value of the holding decreases as the underlying asset price increases. To account for this, the investor's position in asset S in the replicating portfolio also decreases.

When the price of asset S goes down, the value of the long position increases, so the investor takes a larger position in asset S to offset this benefit in their hedging portfolio. The inverse relationship between asset price and asset position is exemplified in the top two plots of Figure 5. When the put option is deep in the money (i.e., asset S is trading well below K), holding the option is financially

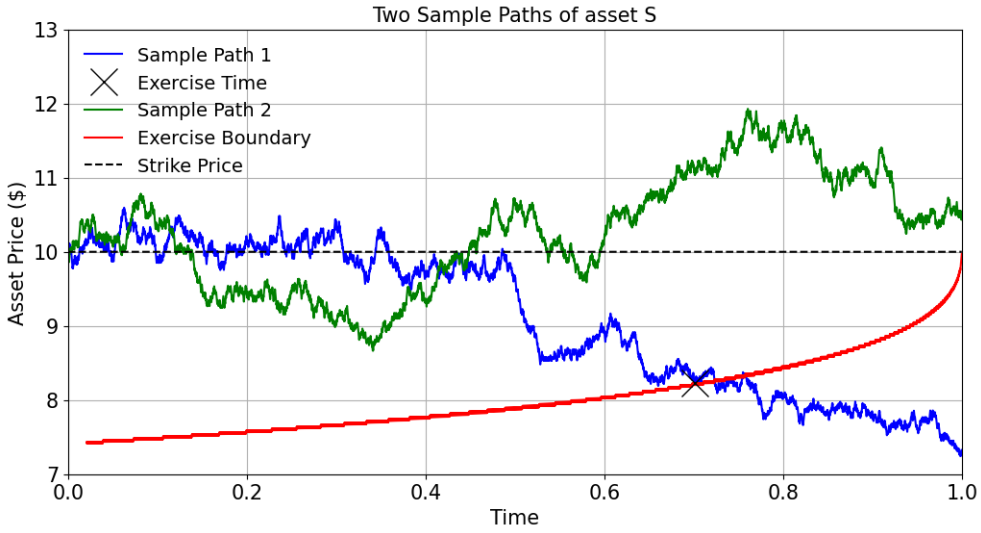

Figure 4: Two Sample Paths of S

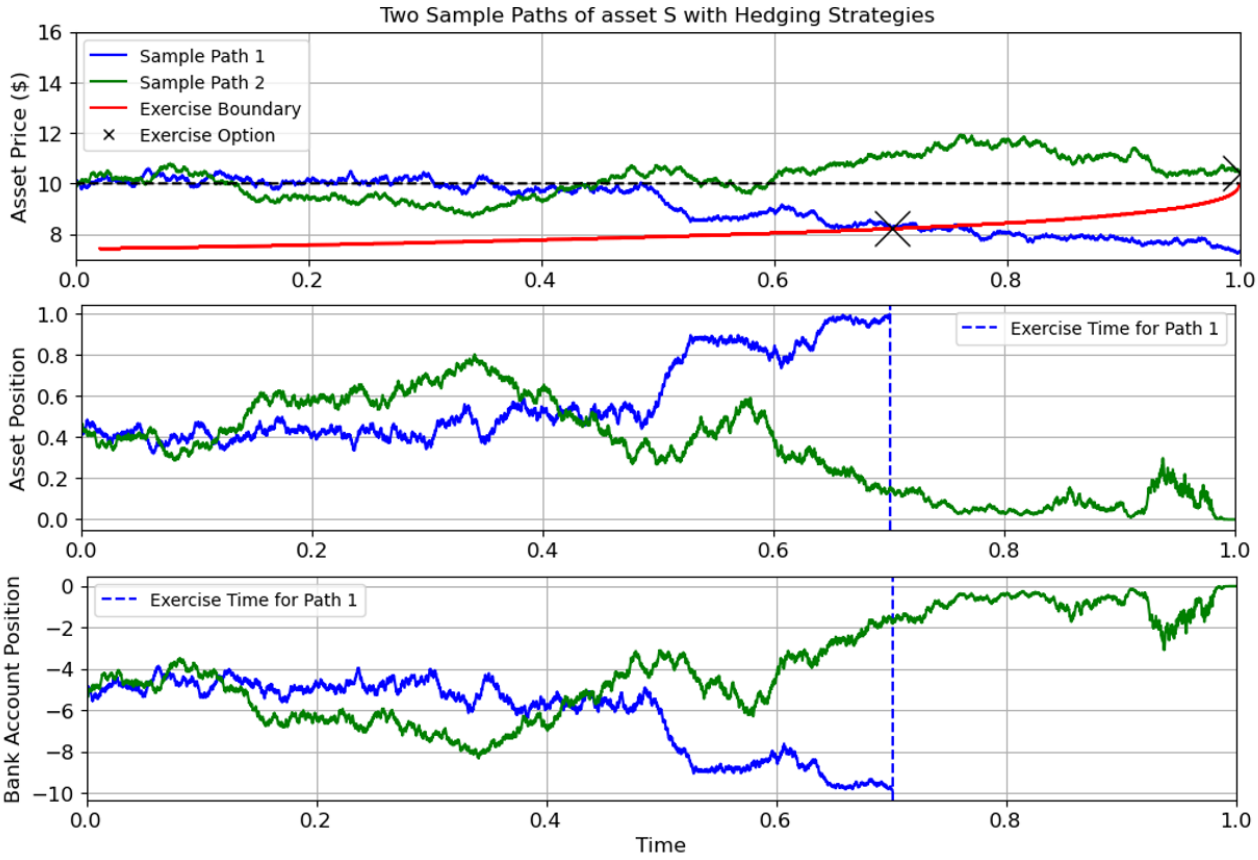

Figure 5: Two Sample Paths of S and the Corresponding Hedging Strategies

equivalent to holding a short position in asset S, so the corresponding position in asset S in the replicating portfolio at the time when exercise is optimal is 1.

To fulfill the strategy's requirement to be self-financing, the investor must also keep a bank account position. Since the investor always has a long position in the put option and the underlying asset S, these positions must be financed by borrowing money (negative bank account position). As shown in path 1 (blue), when the asset price declines and the asset S position is increased, the bank account position decreases as the investor is required to borrow more money. Note also that when the option is exercised in path 1, the positions taken in the asset and the bank account are liberated, as the option is no longer in the investor's portfolio. This is shown by the dashed line at the time of exercise on path 1.

Impact of Market Parameters

Market parameters such as volatility, σ, and risk-free rate, r, have an impact on exercise decisions and trading strategies. These effects are illustrated by performing a pairwise parametric sweep of the path simulation with volatilities of $\sigma = [0.1, 0.2, 0.3]$ and rates of $r = [0.00, 0.02, 0.04]$. The 9 pairwise plots of asset paths and exercise boundaries are shown in Figure 6. The remaining parameters remain unchanged from the previous figure.

Looking first at the simulated asset paths, it is evident as one moves through the columns that the maximum and minimum prices of asset S diverge (i.e., prices are more volatile). Recalling that $S_{t_k} = S_{t_{k-1}} e^{r\Delta t + \sigma\sqrt{\Delta t}\epsilon_k}$, this is an expected result, as the Bernoulli random variable ϵ_k is scaled by the volatility σ in the asset path generation process. The increased volatility also has the effect of pushing down the exercise boundaries. Due to this larger divergence of possible paths of asset S, options have higher potential of being deeper in the money. Thus, the value of holding the option increases, which means that a lower asset price is required for early exercise to be optimal.

The difference in asset paths is much less noticeable for changes in r. However, it is evident that setting $r = 0$ has a large impact on the exercise boundary, as shown in the top row of plots in Figure 6. When the risk-free rate is 0%, the exercise boundary becomes practically non-existent except for the final few time-steps. This makes intuitive sense, as there is little motivation to prematurely exercise the option and deposit the resulting payout into a bank account that yields no return. From the bottom two rows of the figure, it is clear that for the same volatility the exercise boundary is higher for higher risk-free rates. As hedging a long position in the option requires a short position in the bank account, there is less incentive to continue holding in the money options when the cost of borrowing is increased.

The impact of volatility and risk-free rate is further exemplified when examining the change in which they induce on put option prices, as shown in Table 1. When market volatility increases, option prices rise as (assuming all other factors held constant). As discussed, heightened volatility introduces more uncertainty and greater price swings, increasing the expected payout and making options more attractive to investors. Consequently, option sellers demand a higher premium to account for the heightened risk involved. Conversely, when interest rates rise, option prices typically decrease. This is because higher interest rates make other low-risk investments more appealing, reducing the attractiveness of options which are significantly riskier.

Figure 7 shows the positions in the underlying asset S for a hedging portfolio under the same parameter settings as Figure 6. When holding the risk-free rate fixed, it appears that the hedging strategies are very similar for different volatilities when the option is exercised (blue path). For the

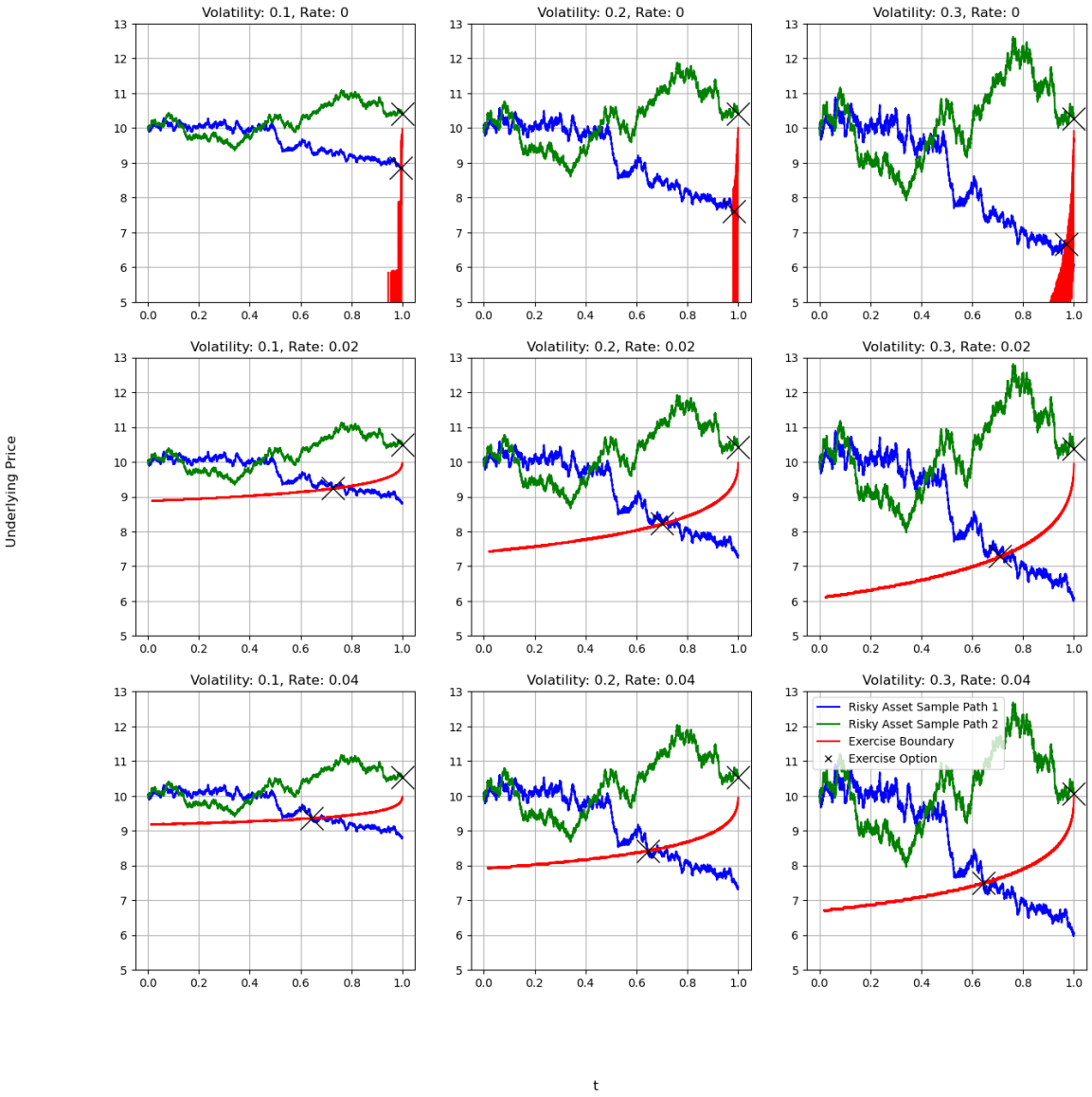

Figure 6: Asset Paths and Exercise Boundaries: Parametric Sweep on Volatility and Risk-Free Rate

Risk-Free Rate, r	Volatility, σ	0.1	0.2	0.3
0.00		\$0.40	\$0.79	\$1.19
0.02		\$0.32	\$0.71	\$1.10
0.04		\$0.27	\$0.64	\$1.03

Table 1: Option Prices at Different Risk-Free Rates and Volatilities

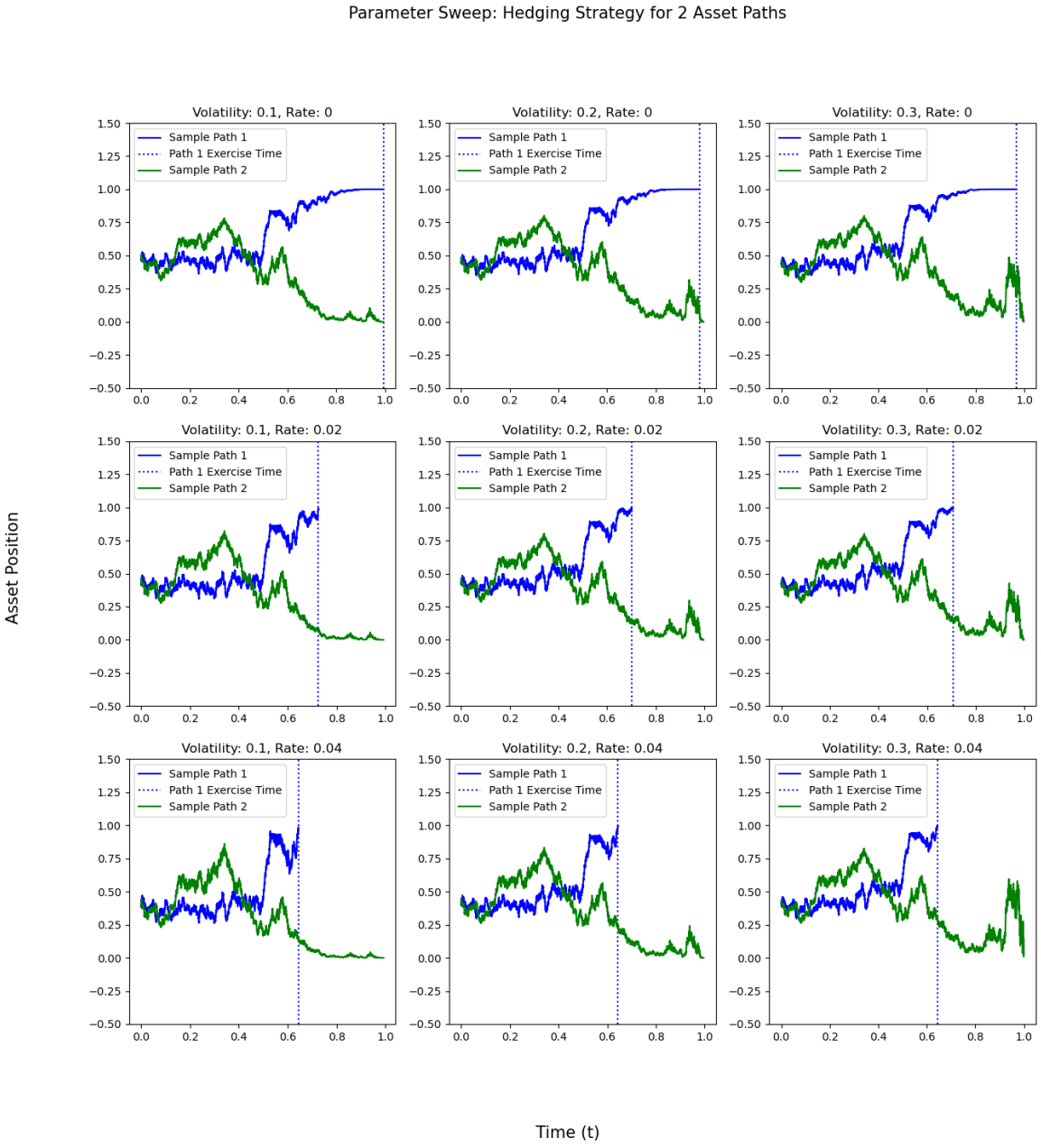

Figure 7: Asset S Position in Hedging Portfolio at Different Risk-Free Rates and Volatilities

option that is not exercised (the green path), changing only the volatility does not have a noticeable impact on hedging strategies for times in the interval [0,0.8]. However, the curves begin to become noticeably different in the period shortly before the option expires (approximately on the interval [0.8,1]). For lower volatilities, the curve decays to zero with few noticeable spikes in the interval. This makes sense as an out of the money option near expiry with low volatility has a low probability of expiring in the money. Thus, the option value approaches zero near expiry and the underlying asset position in the replicating portfolio also approaches zero. On the other hand, as volatility increases, an out of the money option near expiry has a higher probability of expiring in the money compared to an otherwise equivalent option with lower volatility. Thus, the option has more value compared to an otherwise equivalent option with lower volatility and requires a larger position in asset S in the replicating portfolio. This is reflected in the spike in underlying asset position just before expiry when the volatility is 0.2 or 0.3.

When holding the volatility fixed, the changes in the hedging strategies depend on whether the option is exercised. For the option that is exercised (blue path), the optimal early exercise time is earlier for higher interest rates. This is consistent with the observation from Figure 6. For the option that is not exercised (green path), changing risk-free rates have no evident impact on the hedging position in the underlying asset S.

Recall that for the investor to increase their position in the underlying asset S, they must borrow more money. Due to this relationship, the trends in the bank account positions are inverse to the trends in the asset S holding. This is illustrated in Figure 8.

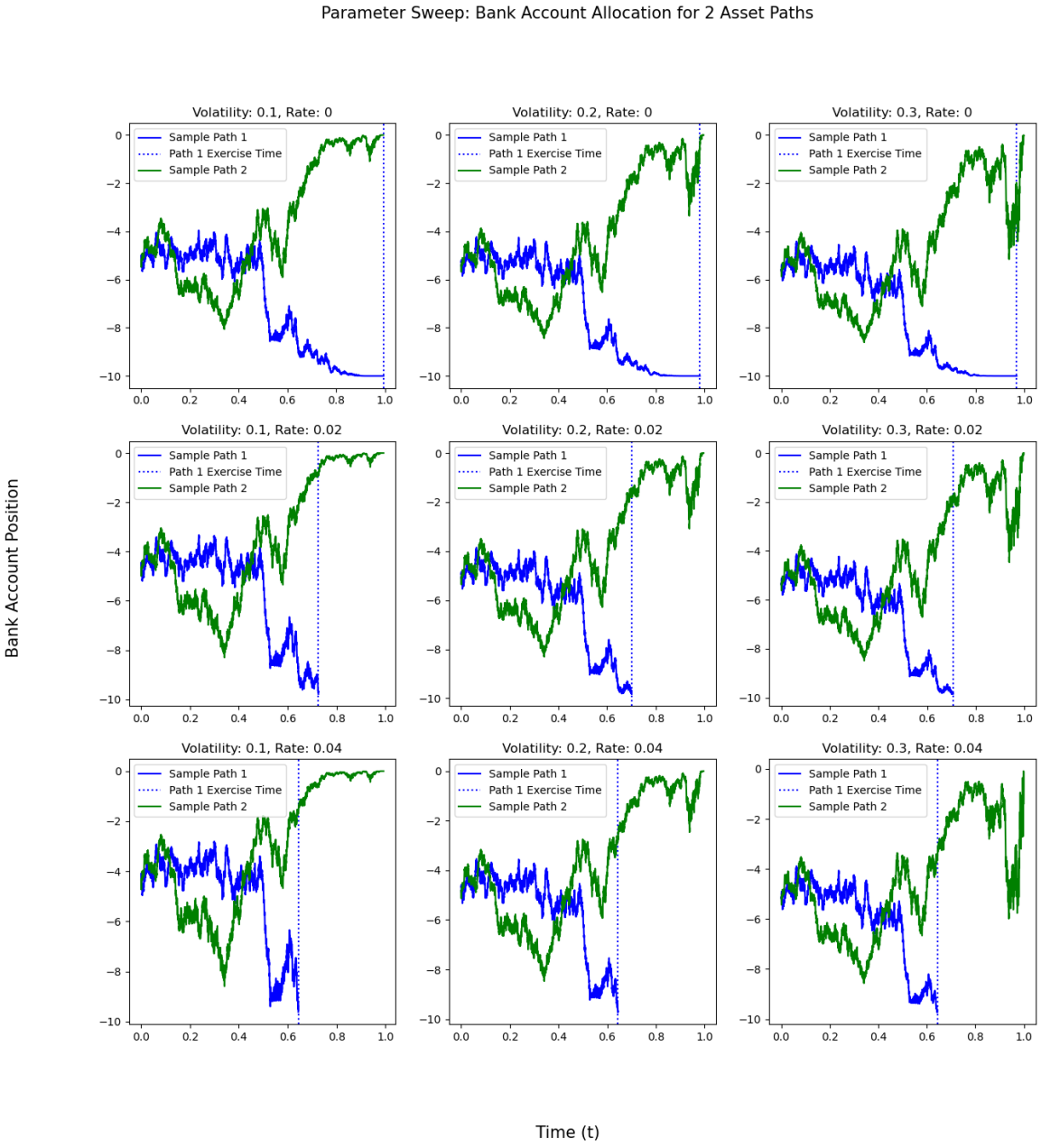

Figure 8: Bank Account Position in Hedging Portfolio at Different Risk-Free Rates and Volatilities

An Early Exercise Case Study

The next part of this analysis consists of an investigation into how profits and stopping times for a holder of an American put option are affected by early exercise. Across 10,000 simulations, the present value of the option holder's profit was recorded for each path that crossed the exercise boundary. The present value is given by $(K - S_t)e^{-rt} - C_0$, where t denotes the exercise time and C_0 is the option premium (paid at time 0 when the option is purchased). The distribution of early exercise profits and stopping times for the case of $N = 5,000, S_0 = \$10.00, K = \$10.00, r = 0.02, \sigma = 0.2, \mu = 0.05$ and $T = 1$ is shown in Figure 9 below. It is noted that for our 10,000 sample paths, 44.81% of options were exercised. The plots do not show the remaining simulations for which the loss is the option premium and the stopping time was maturity, i.e, the distributions are conditioned on early exercised paths.

Looking at Figure 9, the profit distribution (left) mass skews right towards positive present value profit. This makes sense intuitively: investors are more likely to exercise early if the option is in the money. Now looking at the distribution of exercise times (right), it is shown that most early exercises occur close to expiry (time step 5,000 in this example). This also confirms intuition: investors are less likely to exercise early in the option's life when the underlying asset process has much more time to develop, potentially leading to larger payoffs. It is also worth noting that Figure 9 shows that profit can be negative despite the option being exercised early. This occurs when the option is exercised shortly before expiry, where the expiration boundary converges to the strike price. At these points on the expiration boundary, the intrinsic value of the option is less than the initial premium paid, resulting in negative profit.

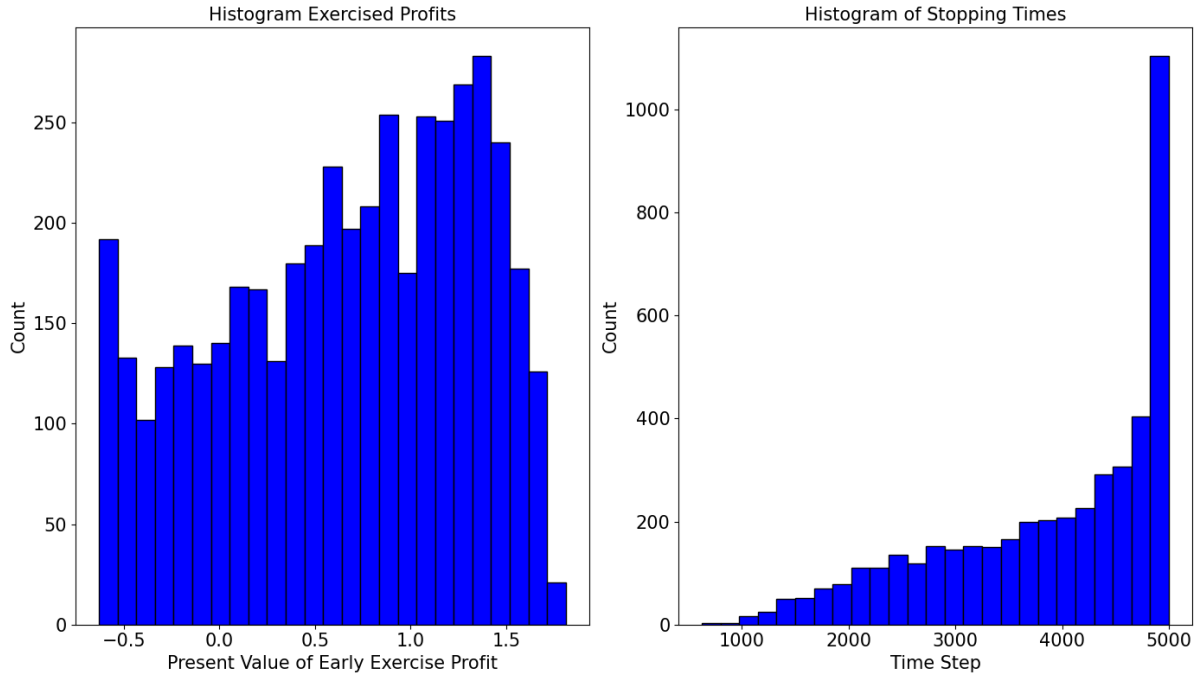

Figure 9: Histogram of Present Value of Early Exercise Profit and Stopping Times Conditioned on Exercise

Impact of Market Parameters on Early Exercise

To determine the impact of market parameters, a parametric sweep of the exercise above was computed. 10000 sample paths were generated with volatilities of $\sigma = [0.1, 0.2, 0.3]$ and risk-free rates of $r = [0.00, 0.02, 0.04]$. The remaining parameters remain unchanged from the previous subsection. For each pairwise parameter combination and sample path, the exercise time was recorded and the present value of the profit for the option holder was computed using the same formula as the previous subsection. Conditional on paths that were exercised, the profit distributions are plotted for each pairwise parameter combination in Figure 10. The stopping time distributions are shown in Figure 11.

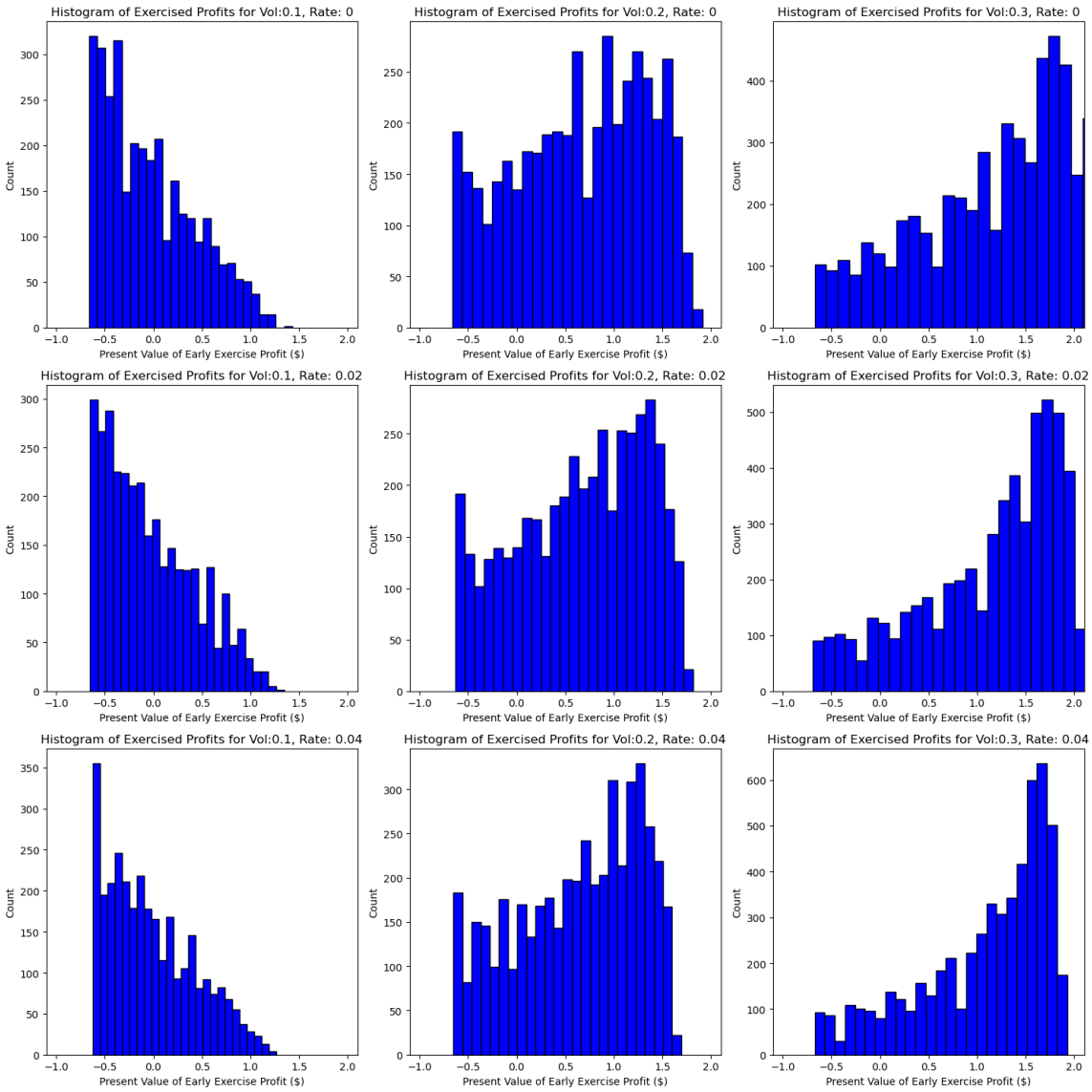

Figure 10: Histogram of Present Value of Early Exercise Profit for Different Volatilities and Risk Free Rates Conditioned on Exercise

First, looking at the impact of increased volatility as one moves through the Figure 10 column-wise,

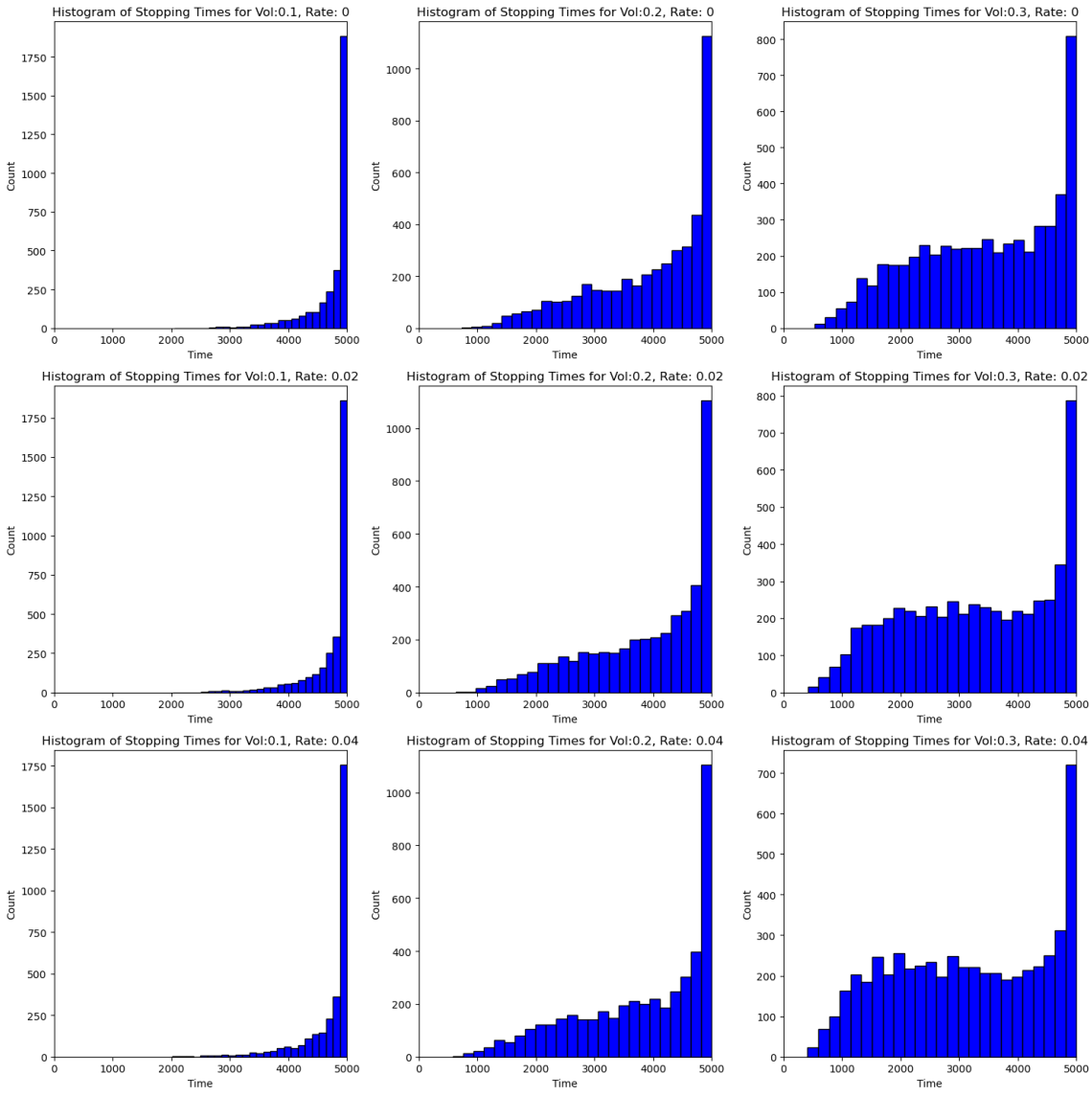

Figure 11: Histogram of Stopping Times for Different Volatilities and Risk Free Rates Conditioned on Exercise

a clear take away is that the right tail of the profit distribution is extended for increased volatility. This result aligns with what was found in the parametric sweep of the exercise boundaries. When volatility is higher, larger changes in the underlying asset price occur, resulting in more opportunities for higher early exercise profit. Due to these higher price swings, the distribution of stopping times also has more mass at earlier time steps for higher volatility.

As for the effect of interest rates, moving row-wise through Figure 10 one can see that the potential for larger profits decreases as the rate increases. When interest rates are at lower levels, investors tend to have less urgency to exercise their options prematurely. Their preference is to exercise only when potential profits are more substantial. In contrast, when interest rates are higher, investors become more inclined to exercise their options earlier. This is because they can redirect their funds into interest-bearing accounts offering higher yields. Consequently, the inclination to exercise at less-optimal profit points becomes more pronounced, as the opportunity cost of holding the option increases in a higher interest rate environment. Figure 11 confirms this results and shows that when rates decrease, investors tend to exercise later.

A final exercise is to examine how an investor's early exercise profit and stopping time varies if the option is purchased at one volatility and the price process evolves at another. Consider an investor that has purchased an American put option on asset S, priced with a volatility 0.2 and interest rate 0.02. Furthermore, let exercise decisions be made using the exercise boundary constructed with this volatility-rate pair. The price process for asset S was then simulated 10000 times for each of $\sigma = [0.1, 0.15, 0.25, 0.3]$, and the early exercise profit and stopping time distributions were computed, as shown in Figures 12 and 13, noting that distributions are conditional on paths that resulted in early exercise.

Figure 12 illustrates that when the process volatility is lower than the purchase and exercise boundary volatility, as seen in the top row, there is higher mass for negative profits. Recall from Table 1 that increasing the volatility increases the option price. Thus, in the top row of Figure 12, the option is overpriced and it is harder to realize a positive profit. Furthermore, since lower volatilities tend to push the exercise boundary upwards, using a 20% volatility boundary results in sub-optimal exercise times, further contributing to the negative profit mass.

Conversely, when simulating a process with higher volatilities than those used for pricing the option and constructing the exercise boundary, a different pattern emerges. In this scenario, the distribution of early exercise profits has more mass in the region with positive profit. This trend occurs because the option is initially priced lower, assuming lower asset S variance, but the simulations reveal greater volatility. In this case, the computed exercise boundary based on the lower volatility assumption is still sub-optimal as it fails to adapt to the higher realized volatilities in the simulation. As depicted in the Figure 13, investors tend to exercise the option earlier in these cases, as the exercise boundary is higher than what it should be. This shows that it is of great interest to investors to purchase options priced at lower volatilities than than those realized in the market, i.e., going long volatiltiy when they feel the volaitilies used in pricing options are too low.

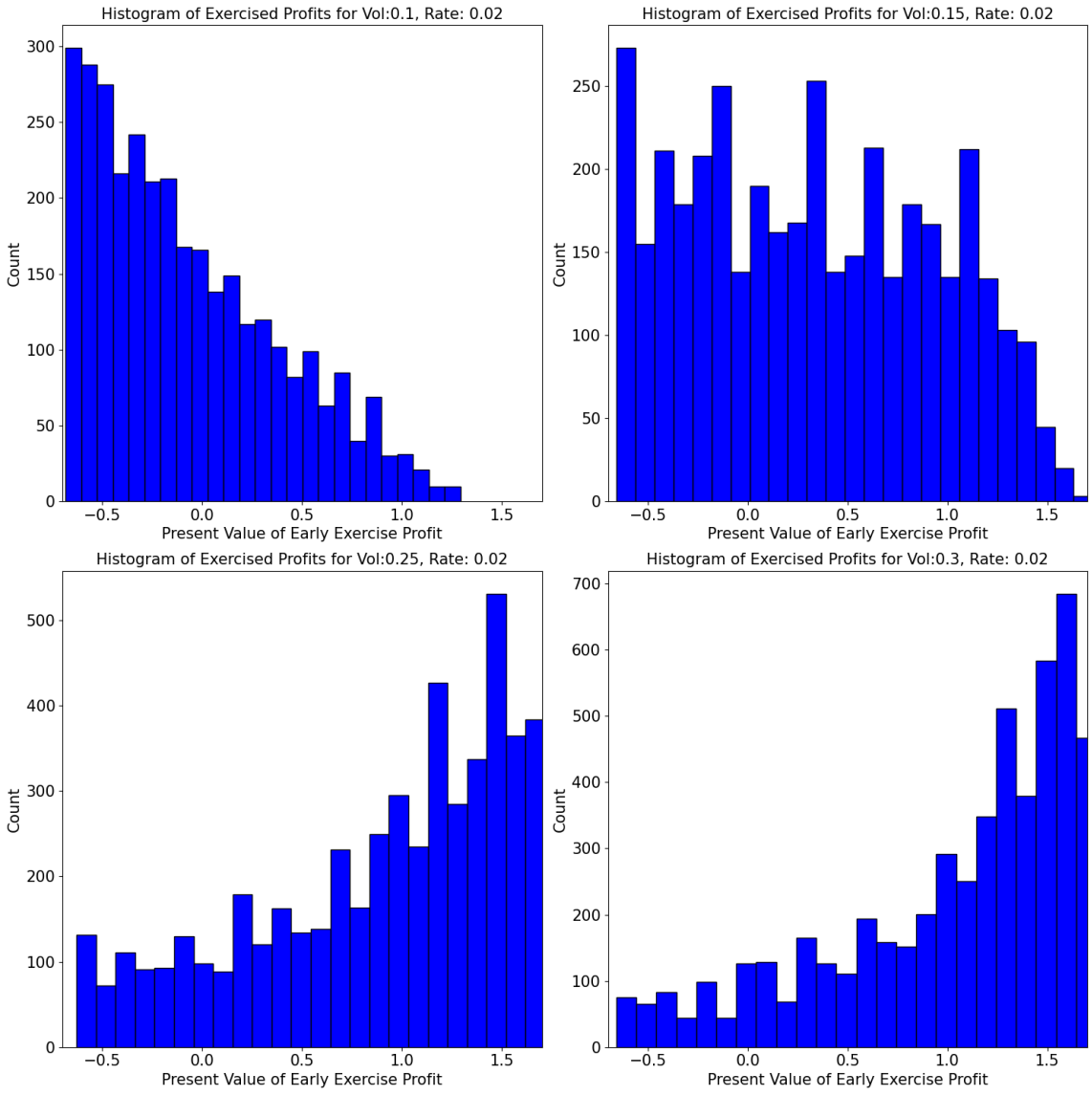

Figure 12: Histogram of Present Value of Profit when Option is Priced at a Different Volatility Conditioned on Exercise

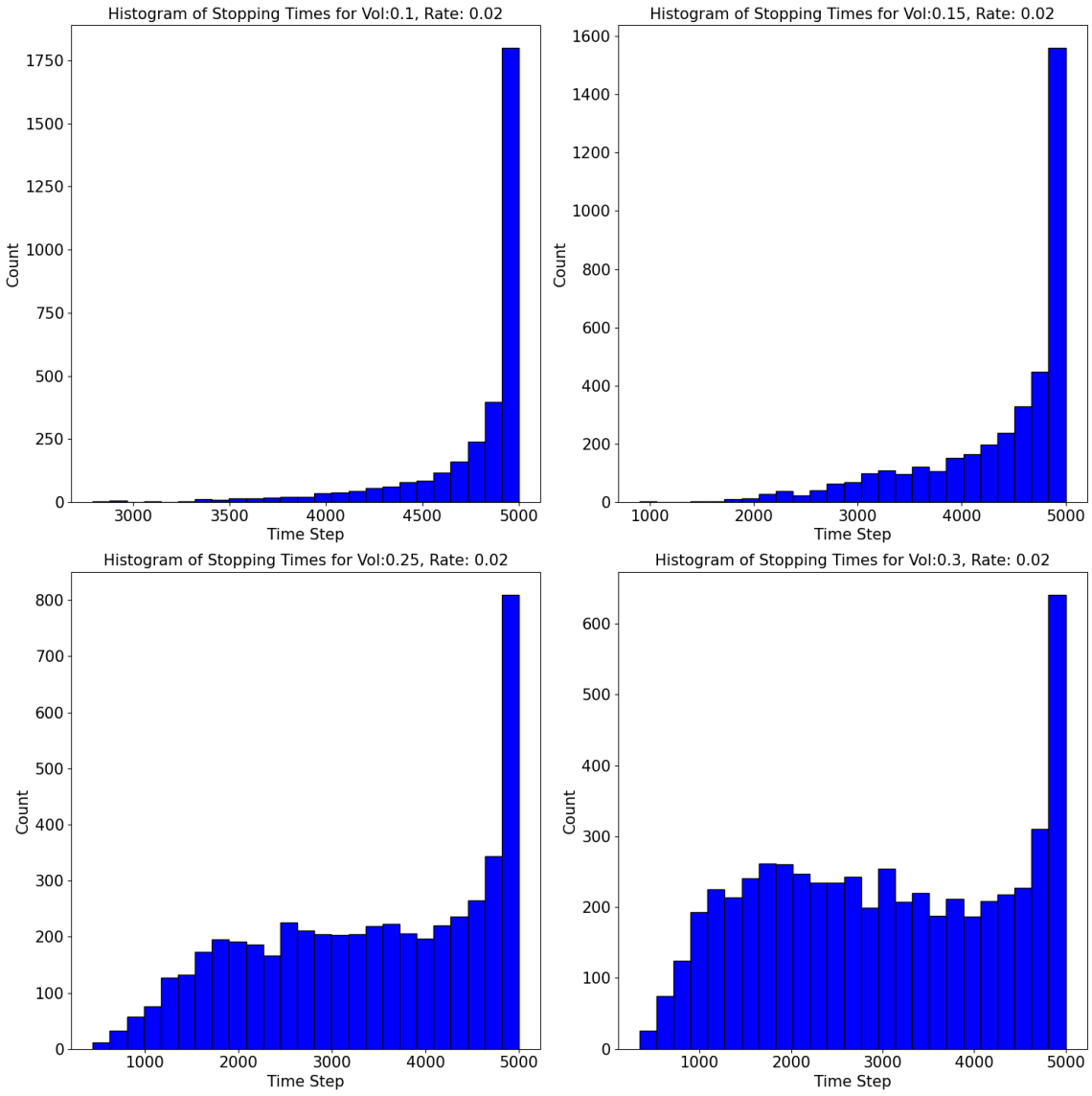

Figure 13: Histogram of Stopping Time when Option is Priced at a Different Volatility Conditioned on Exercise

Part 3: Conclusions

The initial substantial section of this report was dedicated to the derivation of two distinct martingale measures employed for the pricing of American put options. The first measure was predicated on the assumption that a constant interest rate bank account serves as the numeraire, while the second measure was founded on the premise that the numeraire is the underlying risky asset, denoted as S. Additionally, a set of equations was presented, and it was shown that its solution lead to an optimal hedging portfolio for an American put option. Further, it was proven that as the number of time steps approaches infinity, the logarithmic returns tend to converge toward a normal distribution characterized by a mean of rT and a variance of $\sigma^2 T$.

In the second major section, an exploration was undertaken regarding the properties of an American put option through the utilization of Python-based simulations. Initiated with the application of the backward induction procedure, the equivalence of the two previously outlined martingale measures was subsequently confirmed. Following this, the intricacies of hedging strategies for two distinct option paths were shown. Several significant conclusions emerged from this analysis. Primarily, it became apparent that the position in the underlying asset displays an inverse correlation with the underlying asset price: it ascends as the underlying asset price declines. Furthermore, our examination encompassed an exploration of the effects of variations in the risk-free interest rate and asset volatility on the outcomes. The results showed that heightened levels of underlying asset volatility were associated with an increase in the option's price, along with a concurrent reduction in the exercise boundary. Conversely, an increase in risk-free rate was shown to devalue the option, and heighten the exercise boundary.

The report proceeded to examine the distributions of profit and stopping time for an option holder, and it is concluded that in cases where the option is correctly priced, optimal exercising typically yields a positive profit, with a majority of the mass within the stopping time distribution concentrated in proximity to the option's expiry. Furthermore, an investigation was conducted into the influence of market parameters on early exercise resulting in a conclusion in agreement with the parametric sweep of the preceding section: with higher volatilities, the profit has more positive mass and the stopping time distribution exhibits a greater concentration of mass in the earlier time steps. It was once again shown the opposite is true when increasing risk-free rates.

Lastly, a scenario was considered in which the underlying asset's volatility diverged from the volatility employed in the pricing of the option and decision-making process. It was deduced that in instances where the actual volatility of the underlying asset surpasses the one utilized for option pricing, the likelihood of the option holder achieving a positive profit is increased.

Appendix

Please note that all theory references the STA2503 course notes.

Contribution Attestation

We attest that all members in the group made fair contributions to the assignment. The contributions made by each member are as follows:

Brandon: Wrote code for Q2b, derived distribution of log returns, wrote conclusion section of report and compiled all of group members' report writing into Latex file.

Reilly: Wrote initial code structure for exercise boundaries. Compiled all code and prepared all figures for the report. Wrote the theory section (aside from log returns). For Q2a, wrote the section on implementation of exercise boundaries, hedging strategy, and parametric sweep. For Q2b, wrote section on impact of market parameters and impact of mispriced option. Performed final edits on document.

Willem: Derived the Martingale measures for Q1, and the appropriate portfolio replication strategy for Q2a. Wrote code for Q2a, including generating pricing trees, exercise boundaries, sample paths and hedging strategies. Wrote initial abstract and introduction, and performed edits on document.

In addition to the contributions above, all group members actively contributed to the editing of the code and report.

Signatures:

Brandon Tam

Reilly Pickard

Willem Atack